Applied Mathematics and Computation 321 (2018) 49–62

Contents lists available at ScienceDirect

Applied Mathematics and Computation

journal homepage: www.elsevier.com/locate/amc

Two dimensional Riemann problem for a 2×2 system of hyperbolic conservation laws involving three constant states

Jinah Hwang[a], Myoungin Shin[c], Suyeon Shin[b], Woonjae Hwang[b,*]

[a] Department of Mathematics, Korea University, Seoul 02841, Republic of Korea
[b] Division of Applied Mathematical Sciences, Korea University, Sejong 30019, Republic of Korea
[c] Department of Mathematics, Naval Academy, Changwon 51704, Republic of Korea

ARTICLE INFO

MSC:
35L65
35L67
76L15

Keywords:
Riemann problem
Conservation laws
Delta shock

ABSTRACT

Zhang and Zheng (1990) conjectured on the structure of a solution for a two-dimensional Riemann problem for Euler equation. To resolve this illuminating conjecture, many researchers have studied the simplified 2×2 systems. In this paper, 3-pieces Riemann problem for two-dimensional 2×2 hyperbolic system is considered without the restriction that each jump of the initial data projects one planar elementary wave. We classify twelve topologically distinct solutions and construct analytical and numerical solutions. The computed numerical solutions clearly confirm the constructed analytic solutions.

1. Introduction

In 1990, Zhang and Zheng [15] conjectured on the structure of a solution for a four quadrant Riemann problem for two-dimensional $(2-D)$ gas dynamics system:

$$\begin{cases} \rho_t + (\rho u)_x + (\rho v)_y = 0, \\ (\rho u)_t + (\rho u^2 + p)_x + (\rho uv)_y = 0, \\ (\rho v)_t + (\rho uv)_x + (\rho v^2 + p)_y = 0, \end{cases} \tag{1}$$

for the isentropic flow

$$p = A\rho^\gamma,\ \gamma > 1,\ A > 0,$$

and for the adiabatic flow

$$\left(\rho\left(e + \frac{u^2+v^2}{2}\right)\right)_t + \left(\rho u\left(h + \frac{u^2+v^2}{2}\right)\right)_x + \left(\rho v\left(h + \frac{u^2+v^2}{2}\right)\right)_y = 0,$$

$$e = \frac{p}{(\gamma-1)\rho}, \quad h = e + \frac{p}{\rho}.$$

They considered one planar elementary wave for each jump in the initial discontinuity. To resolve this conjecture, many studies have been developed for simplified systems [4].

* Corresponding author.
E-mail addresses: jinahwang@korea.ac.kr (J. Hwang), myoungin@navy.ac.kr (M. Shin), angelic52@korea.ac.kr (S. Shin), woonjae@korea.ac.kr (W. Hwang).

https://doi.org/10.1016/j.amc.2017.10.045
0096-3003/

Tan and Zhang considered the four quadrants Riemann problem for the following 2-D system of conservation laws:

$$\begin{cases} u_t + (u^2)_x + (uv)_y = 0, \\ v_t + (uv)_x + (v^2)_y = 0. \end{cases} \tag{2}$$

They constructed the global solutions for a system (2) in case of the four contact discontinuities initial data [12] and also with the initial data involving shocks, rarefaction waves and contact discontinuities [13]. In this model, a non-classical wave, called as delta shock, appears in some solutions [14].

Instead of four quadrants, Pang et al. considered the three constant initial data separated by x-positive, y-positive and x-negative axes for the system (2). They constructed the solution for the cases of the initial waves involving shocks, rarefactions and contact discontinuities [5], and also for the case with initial data projecting exactly three contact discontinuities [6]. Shen included the case involving exactly one delta shock [8].

In 2003, Hwang and Lindquist removed for the first time the restriction that each jump of the initial data projects one elementary wave. They considered a 2-D Riemann problem for a 2×2 hyperbolic system (3) which is applicable to the polymer flooding of an oil reservoir.

$$\begin{cases} s_t + f^A(s,c)_x + f^B(s,c)_y = 0, \\ (cs)_t + (cf^A(s,c))_x + (cf^B(s,c))_y = 0, \end{cases} \tag{3}$$

where

$$\begin{cases} f^A(s,c) = s^2[1 + A(1-c)(1-s)], & 0 < A < 1/2, \\ f^B(s,c) = s^2[1 + B(1-c)(1-s)], & 0 < B < 1/2. \end{cases} \tag{4}$$

For an isotropic case ($f^A = f^B$), they constructed the solution for a single quadrant (2-pieces) Riemann problem and a four quadrant (4-pieces) Riemann problem by applying two different methods: a transformation into one-dimensional problem, and a direct method by generalized characteristic analysis [1]. For an anisotropic case ($f^A \neq f^B$), they classified twelve topologically distinct solution and constructed the solution for a single quadrant Riemann problem [2]. Pang and Yang constructed the solution of the 2-D Riemann problem for a hyperbolic system (3) involving three contact discontinuities [7].

Sun constructed the solution of the 2-D four quadrant Riemann problem for a non-strictly hyperbolic system (5) of conservation laws without the restriction that each jump of the initial data projects one planar elementary wave:

$$\begin{cases} \rho_t + (\rho u)_x + (\rho u)_y = 0, \\ u_t + (\frac{u^2}{2})_x + (\frac{u^2}{2})_y = 0. \end{cases} \tag{5}$$

They classified and constructed six topologically distinct solutions, in which the delta shock and the vacuum states appear [11].

Shen et al. classified and constructed ten topologically distinct solutions of the 2-D four quadrant Riemann problem for a hyperbolic system (6) of conservation laws without the restriction that each jump of the initial data projects one planar elementary wave:

$$\begin{cases} u_t + (u^2)_x + (u^2)_y = 0, \\ \rho_t + (\rho u)_x + (\rho u)_y = 0. \end{cases} \tag{6}$$

Since this is an isotropic case $(f = g)$, they only considered interactions in $y > x$ plane by using symmetry [9].

In this paper, we consider 2-D Riemann problem for hyperbolic system (6) with three constant initial condition

$$(u, \rho)(0, x, y) = \begin{cases} (u_1, \rho_1), & x > 0,\ y > 0, \\ (u_2, \rho_2), & x < 0,\ y > 0, \\ (u_3, \rho_3), & otherwise. \end{cases} \tag{7}$$

We also remove the restriction that each jump of the initial data projects one planar elementary wave. A 2-D direct construction method is applied in the whole plane, since this problem involves wave interactions from three initial discontinuities and also in order to compare analytic and numerical solutions.

Preliminaries are given in Section 2. We briefly describe the numerical method in Section 3. In Section 4, the initial data are formally classified as 24 cases which resulted in twelve topologically distinct solutions. Finally, the analytic and numerical solutions are constructed in Section 5 and numerical solutions clearly confirm the constructed analytic solutions.

2. Preliminaries

In this section, the basic properties of the system (6) is described. Under the change of variables $\xi = x/t$, $\eta = y/t$, (6) has the self-similar form

$$\begin{cases} -\xi u_\xi - \eta u_\eta + (u^2)_\xi + (u^2)_\eta = 0, \\ -\xi \rho_\xi - \eta \rho_\eta + (\rho u)_\xi + (\rho u)_\eta = 0. \end{cases} \tag{8}$$

The system (8) has two eigenvalues

$$\lambda_1 = \frac{u-\eta}{u-\xi}, \quad \lambda_2 = \frac{2u-\eta}{2u-\xi}, \tag{9}$$

and the corresponding right eigenvectors are

$$r_1 = (0,1)^T, \qquad r_2 = (u,\rho)^T.$$

Then the λ_1 field is linearly degenerate and the λ_2 field is genuinely non-linear if $\eta \neq \xi$ and $u \neq 0$, because $\nabla\lambda_1 \cdot r_1 \equiv 0$ and $\nabla\lambda_2 \cdot r_2 \neq 0$ for $\eta \neq \xi$ and $u \neq 0$.

• *Contact discontinuity*

For a smooth bounded discontinuity $\eta = \eta(\xi)$ with (u_1, ρ_1) and (u_2, ρ_2) on each side, we solve the following Rankine–Hugoniot condition

$$\begin{cases} (\eta - \xi\sigma, \sigma, -1) \cdot ([u], [u^2], [u^2]) = 0, \\ (\eta - \xi\sigma, \sigma, -1) \cdot ([\rho], [\rho u], [\rho u]) = 0, \end{cases} \tag{10}$$

where $[u] = u_1 - u_2$ to obtain

$$\frac{d\eta}{d\xi} = \sigma = \frac{\eta - u_1}{\xi - u_1} = \frac{\eta - u_2}{\xi - u_2}. \tag{11}$$

This is a contact discontinuity and the integral curve of (10) comes from infinity and ends at the singular point $(u_1, u_1) = (u_2, u_2)$. For the contact discontinuity $J(\xi)$, which is parallel to ξ-axis, $J(\xi)$ satisfies

$$J(\xi) \ : \ \xi = u_1 = u_2. \tag{12}$$

• *Shock wave*

We solve the Eq. (10) to obtain

$$\frac{d\eta}{d\xi} = \sigma = \frac{\eta - (u_1 + u_2)}{\xi - (u_1 + u_2)}, \quad \frac{\rho_1}{u_1} = \frac{\rho_2}{u_2}. \tag{13}$$

The shock satisfies Eq. (13) and the entropy condition. The entropy condition is defined by

$$\begin{cases} \lambda_i(u_2;\xi,\eta) < \sigma < \lambda_i(u_1;\xi,\eta), \\ \qquad\qquad\qquad\qquad\qquad\qquad i = 1,2 \\ \lambda_{i-1}(u_1;\xi,\eta) < \sigma < \lambda_{i+1}(u_2;\xi,\eta), \end{cases} \tag{14}$$

which means that three characteristic lines are “incoming” and the remaining one “outoing”. The integral curve of $d\eta/d\xi = \sigma$ comes from infinity and ends at the singular point $(\xi, \eta) = (u_1 + u_2, u_1 + u_2)$. For the shock $S(\xi)$, which is parallel to ξ-axis, $S(\xi)$ satisfies

$$S(\xi) \ : \ \xi = u_1 + u_2, \quad \frac{\rho_2}{u_2} = \frac{\rho_1}{u_1}, \quad 0 < u_1 < u_2 \ \text{ or } \ u_1 < u_2 < 0. \tag{15}$$

• *Rarefaction wave*

We can get the left eigenvectors of λ:

$$l_1 = (-\rho, u), \qquad l_2 = (1, 0).$$

By multiplying left eigenvectors to each equation in (8) respectively, (8) is reduced to

$$\begin{cases} \left(\frac{\rho}{u}\right)_\xi + \lambda_1 \left(\frac{\rho}{u}\right)_\eta = 0, \\ u_\xi + \lambda_2 u_\eta = 0. \end{cases} \tag{16}$$

The second equation of (16) implies that the characteristic line is a straight line. Suppose (u_0, ρ_0) is the intersection point of the second characteristic line and the base curve $\eta = \xi$ and (u, ρ) is the value of the solution at the point (ξ, η). Then we have

$$\begin{cases} \dfrac{d\eta}{d\xi} = \dfrac{2u - \eta}{2u - \xi} = \dfrac{\rho_0 - \eta}{u_0 - \xi}, \\ \dfrac{\rho}{u} = \dfrac{\rho_0}{u_0}, \end{cases} \tag{17}$$

which shows that the second characteristic is toward $(2u, 2u)$. For the rarefaction wave $R(\xi)$, which is parallel to ξ-axis, $R(\xi)$ satisfies

$$R(\xi) \ : \ \xi = 2u, \quad \frac{\rho}{u} = \frac{\rho_1}{u_1}, \ u_2 \leq u \leq u_1. \tag{18}$$

• *Delta shock*

We define a three-dimensional weighted delta function $\omega(t, s)\delta_S$ supported on a smooth surface S parameterized as $x = x(t, s),\ y = y(t, s)\ (s \geq 0)$, which separates the $(t \geq 0,\ x,\ y)$-space into two parts Ω_1 and Ω_2, by

$$< \omega(t,s)\delta_S, \phi >= \int_0^{+\infty}\int_0^{+\infty} \omega(t,s)\phi(t,x(t,s),y(t,s))dsdt, \tag{19}$$

for all $\phi \in C_0^\infty([0,+\infty)\times R^2)$. Consider the solution of the form

$$(u,\rho)(t,x,y) = \begin{cases} (u_1,\rho_1) & (t,x,y)\in\Omega_1, \\ (u_\delta(t,s),\omega(t,s)\delta(t,x-x(t,s),y-y(t,s)) & (t,x,y)\in S, \\ (u_2,\rho_2) & (t,x,y)\in\Omega_2 \end{cases} \tag{20}$$

where $\omega(t,s)\in C^1([0,+\infty)\times[0,+\infty))$ and δ is the Dirac measure with support S, $(u_1,\ \rho_1)$ and $(u_2,\ \rho_2)$ are the respective bounded smooth solutions of (6) in Ω_1 and Ω_2.

It is shown in [9] that the solution of (6) in the sense of distribution satisfies

$$\begin{cases} < u,\phi_t > + < u^2,\phi_x > + < u^2,\phi_y >= 0, \\ < \rho,\phi_t > + < \rho u,\phi_x > + < \rho u,\phi_y >= 0, \end{cases} \tag{21}$$

for any $\phi \in C_0^\infty([0,+\infty)\times R^2)$, where

$$\begin{cases} < \rho,\phi >= \int_{\Omega_-}\rho_-\phi dxdydt + \int_{\Omega_+}\rho_+\phi dxdydt + < \omega(t,s)\delta_S,\phi >, \\ < \rho u,\phi >= \int_{\Omega_-}\rho_- u_-\phi dxdydt + \int_{\Omega_+}\rho_+ u_+\phi dxdydt + < u_\delta\omega(t,s)\delta_S,\phi > . \end{cases} \tag{22}$$

$(u,\ \rho)$ given in (20) is the solution of (6) in the sense of distribution if the following generalized Rankine–Hugoniot condition is satisfied

$$\begin{cases} \dfrac{\partial x}{\partial t} = \dfrac{\partial y}{\partial t} = u_\delta(t,s), \\ \big([u],[u^2],[u^2]\big)\cdot(n_t,n_x,n_y) = 0, \\ \dfrac{\partial \omega}{\partial t} = \big([\rho],[\rho u],[\rho u]\big)\cdot(n_t,n_x,n_y) \end{cases} \tag{23}$$

in which $[u] = u_1 - u_2$ is the jump of u across the discontinuity surface S, and the normal of S can be obtained by

$$(n_t,n_x,n_y) = \left(u_\delta\left(\frac{\partial y}{\partial s}-\frac{\partial x}{\partial s}\right), -\frac{\partial y}{\partial s}, \frac{\partial x}{\partial s}\right). \tag{24}$$

The entropy condition of delta shock implies that all characteristics are “incoming” on both sides of the delta-shock and the singular point of delta shock is $(\xi,\eta) = (u_1+u_2, u_1+u_2)$. For the delta shock $S_\delta(\xi)$, which is parallel to ξ-axis, $S_\delta(\xi)$ satisfies

$$S_\delta(\xi)\ :\ \xi = u_1+u_2, \quad u_1 \leq 0 \leq u_2. \tag{25}$$

3. Numerical method

Central scheme offers a simple and versatile approach for computing approximate solutions of nonlinear systems of hyperbolic conservation laws. However, there are numerical dissipations in case of contact discontinuity. To treat numerical dissipations, we briefly describe how we modify semi-discrete central upwind scheme by changing flux functions [3,10]. We first rewrite the system (6) as

$$U_t + f(U)_x + g(U)_y = 0 \tag{26}$$

where

$$U = \begin{bmatrix} u \\ \rho \end{bmatrix}, f(U) = \begin{bmatrix} u^2 \\ \rho u \end{bmatrix}, g(U) = \begin{bmatrix} u^2 \\ \rho u \end{bmatrix}. \tag{27}$$

A second order two dimensional semi-discrete central-upwind scheme can be obtained in the following conservative form:

$$\frac{d}{dt}\bar{U}_{j,k}(t) = -\frac{H^x_{j+\frac12,k}(t) - H^x_{j-\frac12,k}(t)}{\Delta x} - \frac{H^y_{j,k+\frac12}(t) - H^y_{j,k-\frac12}(t)}{\Delta y}. \tag{28}$$

To reduce numerical dissipation, we add anti-diffusion terms $q^x_{j+1/2,k}$ and $q^y_{j,k+1/2}$ to the numerical fluxes $H^x_{j+1/2,k}(t)$ and $H^y_{j,k+1/2}(t)$, respectively.

The second order two dimensional numerical fluxes, H^x and H^y, are

$$
\begin{aligned}
H^x_{j+\frac{1}{2},k}(t) &:= \frac{a^+_{j+\frac{1}{2},k} f(U^E_{j,k}) - a^-_{j+\frac{1}{2},k} f(U^W_{j+1,k})}{a^+_{j+\frac{1}{2},k} - a^-_{j+\frac{1}{2},k}} + a^+_{j+\frac{1}{2},k} a^-_{j+\frac{1}{2},k}\left[\frac{U^W_{j+1,k} - U^E_{j,k}}{a^+_{j+\frac{1}{2},k} - a^-_{j+\frac{1}{2},k}} - q^x_{j+\frac{1}{2},k}\right],\\
H^y_{j,k+\frac{1}{2}}(t) &:= \frac{b^+_{j,k+\frac{1}{2}} g(U^N_{j,k}) - b^-_{j,k+\frac{1}{2}} g(U^S_{j,k+1})}{b^+_{j,k+\frac{1}{2}} - b^-_{j,k+\frac{1}{2}}} + b^+_{j,k+\frac{1}{2}} b^-_{j,k+\frac{1}{2}}\left[\frac{U^S_{j,k+1} - U^N_{j,k}}{b^+_{j,k+\frac{1}{2}} - b^-_{j,k+\frac{1}{2}}} - q^y_{j,k+\frac{1}{2}}\right],
\end{aligned}
\tag{29}
$$

and anti-diffusion terms $q^x_{j+1/2,k}$ and $q^y_{j,k+1/2}$ are

$$
\begin{aligned}
q^x_{j+\frac{1}{2},k} &= \operatorname{minmod}\left(\frac{U^{NW}_{j+1,k} - \omega^{int}_{j+\frac{1}{2},k}}{a^+_{j+\frac{1}{2},k} - a^-_{j+\frac{1}{2},k}}, \frac{U^{SW}_{j+1,k} - \omega^{int}_{j+\frac{1}{2},k}}{a^+_{j+\frac{1}{2},k} - a^-_{j+\frac{1}{2},k}}, \frac{\omega^{int}_{j+\frac{1}{2},k} - U^{NE}_{j,k}}{a^+_{j+\frac{1}{2},k} - a^-_{j+\frac{1}{2},k}}, \frac{\omega^{int}_{j+\frac{1}{2},k} - U^{SE}_{j,k}}{a^+_{j+\frac{1}{2},k} - a^-_{j+\frac{1}{2},k}}\right),\\
q^y_{j,k+\frac{1}{2}} &= \operatorname{minmod}\left(\frac{U^{SW}_{j,k+1} - \omega^{int}_{j,k+\frac{1}{2}}}{b^+_{j,k+\frac{1}{2}} - b^-_{j,k+\frac{1}{2}}}, \frac{U^{SE}_{j,k+1} - \omega^{int}_{j,k+\frac{1}{2}}}{b^+_{j,k+\frac{1}{2}} - b^-_{j,k+\frac{1}{2}}}, \frac{\omega^{int}_{j,k+\frac{1}{2}} - U^{NW}_{j,k}}{b^+_{j,k+\frac{1}{2}} - b^-_{j,k+\frac{1}{2}}}, \frac{\omega^{int}_{j,k+\frac{1}{2}} - U^{NE}_{j,k}}{b^+_{j,k+\frac{1}{2}} - b^-_{j,k+\frac{1}{2}}}\right),
\end{aligned}
\tag{30}
$$

where the intermediate values are:

$$
\begin{aligned}
\omega^{int}_{j+\frac{1}{2},k} &= \frac{a^+_{j+\frac{1}{2},k} U^W_{j+1,k} - a^-_{j+\frac{1}{2},k} U^E_{j,k} - \{f(U^W_{j+1,k}) - f(U^E_{j,k})\}}{a^+_{j+\frac{1}{2},k} - a^-_{j+\frac{1}{2},k}},\\
\omega^{int}_{j,k+\frac{1}{2}} &= \frac{b^+_{j,k+\frac{1}{2}} U^S_{j,k+1} - b^-_{j,k+\frac{1}{2}} U^N_{j,k} - \{g(U^S_{j,k+1}) - g(U^N_{j,k})\}}{b^+_{j,k+\frac{1}{2}} - b^-_{j,k+\frac{1}{2}}}.
\end{aligned}
\tag{31}
$$

The point values $U^{NE}_{j,k}$, $U^{NW}_{j,k}$, $U^{SE}_{j,k}$, $U^{SW}_{j,k}$, $U^E_{j,k}$, $U^W_{j,k}$. $U^S_{j,k}$ and $U^N_{j,k}$ in (29)–(31) are computed from a piecewise linear interpolation reconstruction, $\widetilde{U}(x, y, t) = \sum_{j,k}[\bar{U}^n_{j,k} + (U_x)^n_{j,k}(x - x_j) + (U_y)^n_{j,k}(y - y_k)]\chi_{j,k}(x, y)$ where $\chi_{j,\,k}(x, y)$ is the characteristic function over the corresponding cell $(x_{j-1/2}, x_{j+1/2}) \times (y_{k-1/2}, y_{k+1/2})$ and are given by

$$
\begin{aligned}
&U^{E(W)}_{j,k} := \bar{U}^n_{j,k} \pm \frac{\Delta x}{2}(U_x)^n_{j,k}, \quad U^{N(S)}_{j,k} := \bar{U}^n_{j,k} \pm \frac{\Delta y}{2}(U_y)^n_{j,k},\\
&U^{NE(NW)}_{j,k} := \bar{U}^n_{j,k} \pm \frac{\Delta x}{2}(U_x)^n_{j,k} + \frac{\Delta y}{2}(U_y)^n_{j,k}, \quad U^{SE(SW)}_{j,k} := \bar{U}^n_{j,k} \pm \frac{\Delta x}{2}(U_x)^n_{j,k} - \frac{\Delta y}{2}(U_y)^n_{j,k}.
\end{aligned}
\tag{32}
$$

In the convex case, the one sided local speeds of propagation are calculated by

$$
\begin{aligned}
a^+_{j+\frac{1}{2},k} &:= \max\left\{\lambda_N\left(\frac{\partial f}{\partial U}(U^W_{j+1,k})\right), \lambda_N\left(\frac{\partial f}{\partial U}(U^E_{j,k})\right), 0\right\},\\
a^-_{j+\frac{1}{2},k} &:= \min\left\{\lambda_1\left(\frac{\partial f}{\partial U}(U^W_{j+1,k})\right), \lambda_1\left(\frac{\partial f}{\partial U}(U^E_{j,k})\right), 0\right\},\\
b^+_{j,k+\frac{1}{2}} &:= \max\left\{\lambda_N\left(\frac{\partial g}{\partial U}(U^S_{j,k+1})\right), \lambda_N\left(\frac{\partial g}{\partial U}(U^N_{j,k})\right), 0\right\},\\
b^-_{j,k+\frac{1}{2}} &:= \min\left\{\lambda_1\left(\frac{\partial g}{\partial U}(U^S_{j,k+1})\right), \lambda_1\left(\frac{\partial g}{\partial U}(U^N_{j,k})\right), 0\right\},
\end{aligned}
\tag{33}
$$

where $\lambda_1 < \cdots < \lambda_N$ are the eigenvalues of $\partial f/\partial U$ or $\partial g/\partial U$. Further details can be found in [3,10]. For all computations, in this paper, 600 $\times$ 600 cells are used and the CFL is 0.05. The computational domain is $[-1, 1] \times [-1, 1]$ and t=0.25, $\rho_1 = \rho_2 = \rho_3 = 0.77$.

4. Classification of initial data

Though there are three states u_1, u_2 and u_3, the order of u_1, u_2, u_3 and 0 must be considered because of a delta shock. The entropy condition indicates that all four characteristics are incoming from both sides of the delta shock which means that 0 is between two states. Since the evolution of u does not depend on ρ, initial data can be classified only with u. Thus we have total $4! = 24$ cases. If the exterior waves which come from positive η-axis, negative ξ-axis and positive ξ-axis are counted in this order, then the cases are classified as:

- *no delta shock*

$$3S\Big\{\text{Case 1 : } JS + JS + SJ\ (u_1 < u_2 < u_3 < 0),\ SJ + SJ + JS\ (0 < u_1 < u_2 < u_3)$$

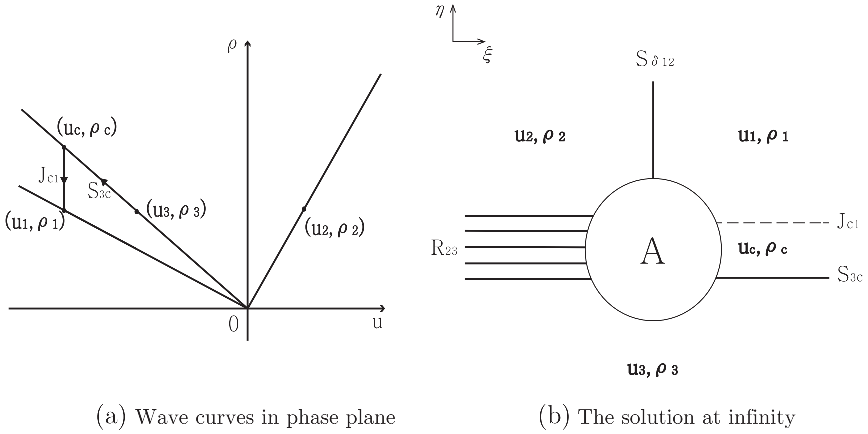

(a) Wave curves in phase plane (b) The solution at infinity

Fig. 1. Construction of the solutions.

$$2S\begin{cases}\text{Case 2 }: JR+JS+SJ\ (u_2<u_1<u_3<0),\ SJ+RJ+JS\ (0<u_1<u_3<u_2)\\ \text{Case 3 }: RJ+SJ+JS\ (0<u_2<u_1<u_3),\ JS+JR+SJ\ (u_1<u_3<u_2<0)\end{cases}$$

$$1S\begin{cases}\text{Case 4 }: JR+JS+RJ\ (u_2<u_3<u_1<0),\ SJ+RJ+JR\ (0<u_3<u_1<u_2)\\ \text{Case 5 }: R+JS+R\ \ (u_2<u_3<0<u_1),\ SJ+R+R\quad (u_3<0<u_1<u_2)\\ \text{Case 6 }: RJ+SJ+JR\ (0<u_2<u_3<u_1),\ JS+JR+RJ\ (u_3<u_1<u_2<0)\end{cases}$$

$$0S\begin{cases}\text{Case 7 }: JR+JR+RJ\ (u_3<u_2<u_1<0),\ RJ+RJ+JR\ (0<u_3<u_2<u_1)\\ \text{Case 8 }: R+JR+R\ \ (u_3<u_2<0<u_1),\ RJ+R+R\quad (u_3<0<u_2<u_1)\end{cases}$$

- *one delta shock*

$$\begin{cases}\text{Case 9 }: S_\delta+R+RJ\ (u_3<u_1<0<u_2),\ R+S_\delta+JR\ (u_2<0<u_3<u_1)\\ \text{Case 10}: S_\delta+R+SJ\ (u_1<u_3<0<u_2),\ R+S_\delta+JS\ (u_2<0<u_1<u_3)\end{cases}$$

- *two delta shocks*

$$\begin{cases}\text{Case 11 }: S_\delta+RJ+S_\delta\ (u_1<0<u_3<u_2),\ JR+S_\delta+S_\delta\ (u_2<u_1<0<u_3)\\ \text{Case 12 }: S_\delta+SJ+S_\delta\ (u_1<0<u_2<u_3),\ JS+S_\delta+S_\delta\ (u_1<u_2<0<u_3)\end{cases}$$

Since the second term has similar structures of the first term for each case, we consider only the first term of each case.

5. Construction of the solution

We remove the restriction that each jump of the initial data projects one planar elementary wave. Then, we obtain one wave or two waves at infinity. If data at the initial discontinuity has the same sign, then two wave solutions at infinity exist, which are either a contact discontinuity and a shock, or a contact discontinuity and a rarefaction wave. If data at the initial discontinuity has different signs, then there is only one wave solution at infinity, which is either a delta shock or a rarefaction wave. For example, Fig. 1(a) shows wave curves in phase plane and Fig. 1(b) shows the solution at infinity, in case of $u_1 < u_3 < 0 < u_2$. There is only one wave which is a delta shock between (u_1, ρ_1) and (u_2, ρ_2) since u_1 and u_2 have different signs. Similarly, there is only one wave which is a rarefaction wave between (u_2, ρ_2) and (u_3, ρ_3) since u_2 and u_3 have different signs. Finally, there are two waves which are a shock and a contact discontinuity between (u_3, ρ_3) and (u_1, ρ_1) since u_3 and u_1 have the same sign. A new state (u_c, ρ_c) is developed between a shock and a contact discontinuity and it satisfies

$$u_c = u_1,\quad \frac{\rho_c}{u_c} = \frac{\rho_3}{u_3} \tag{34}$$

by jump condition. Then the wave interactions in center region A in Fig. 1(b) are determined. Other cases can be constructed similarly. These are investigated in detail on a case-by-case basis.

5.1. No delta shock

5.1.1. Three shock waves

Case 1. $JS+JS+SJ$

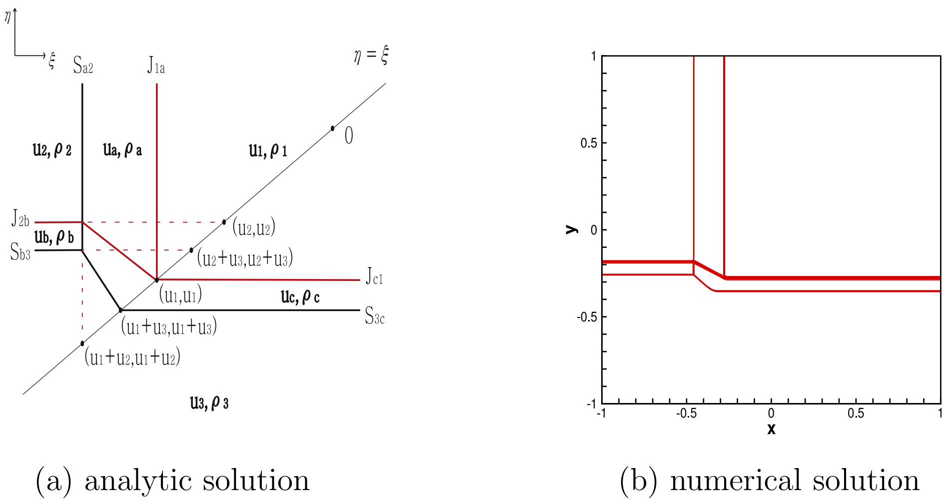

Fig. 2. Case 1. $JS + JS + SJ$ ($u_1 < u_2 < u_3 < 0$).

In this case, the initial states satisfy $u_1 < u_2 < u_3 < 0$. From the initial discontinuity, the contact discontinuity J_{1a} and the shock S_{a2} – which are both parallel to the positive η-axis – and a new state (u_a, ρ_a) between J_{1a} and S_{a2} are formed. The state (u_a, ρ_a) satisfies $u_a = u_1$ and $\frac{\rho_a}{u_a} = \frac{\rho_2}{u_2}$. The contact discontinuity J_{1a} is heading to the point $(\xi, \eta) = (u_1, u_1)$ and the shock S_{a2} is heading to the point $(\xi, \eta) = (u_1 + u_2, u_1 + u_2)$. The contact discontinuity J_{2b} and the shock S_{b3} – which are both parallel to the negative ξ-axis – and a new state (u_b, ρ_b) between J_{2b} and S_{b3} are formed. The state (u_b, ρ_b) satisfies $u_b = u_2$ and $\frac{\rho_b}{u_b} = \frac{\rho_3}{u_3}$. The contact discontinuity J_{2b} is heading to the point (u_2, u_2) and the shock S_{b3} is heading to the point $(u_2 + u_3, u_2 + u_3)$. The shock S_{3c} and the contact discontinuity J_{c1} – which are both parallel to the positive ξ-axis – and a new state (u_c, ρ_c) between S_{3c} and J_{c1} are formed. The state (u_c, ρ_c) satisfies $u_c = u_1$ and $\frac{\rho_c}{u_c} = \frac{\rho_3}{u_3}$. The contact discontinuity J_{c1} is heading to the point (u_1, u_1) and the shock S_{3c} is heading to the point $(u_1 + u_3, u_1 + u_3)$. The contact discontinuity J_{2b} intersects with the shock S_{a2} at the point $(\xi_0, \eta_0) = (u_1 + u_2, u_2)$ and the contact discontinuity J_{ac} satisfies

$$\eta - u_1 = \frac{u_2 - u_1}{u_2}(\xi - u_1). \tag{35}$$

This contact discontinuity ends at the singular point (u_1, u_1) that equals to the singular point of J_{c1}. So, they meet at the point (u_1, u_1). The shock $S_{cb}(= S_{a2})$ intersects with S_{b3} at the point $(u_1 + u_2, u_2 + u_3)$, then the shock S_{c3} which is expressed as

$$\eta - (u_1 + u_3) = \frac{u_2 - u_1}{u_2 - u_3}(\xi - (u_1 + u_3)) \tag{36}$$

meets S_{3c} at the same singular point $(u_1 + u_3, u_1 + u_3)$. The analytic solution and the numerical solution are shown in Fig. 2(a) and (b), respectively. The numerical solution confirms the constructed analytic solution. The initial condition for this case is $u_1 = -0.56$, $u_2 = -0.37$, $u_3 = -0.15$.

5.1.2. Two shock waves

Case 2. JR + JS + SJ

In this case, the initial states satisfy $u_2 < u_1 < u_3 < 0$. From the initial discontinuity, the contact discontinuity J_{1a} and the rarefaction wave R_{a2} – which are both parallel to the positive η-axis – and a new state (u_a, ρ_a) between J_{1a} and R_{a2} are formed. The state (u_a, ρ_a) satisfies $u_a = u_1$ and $\frac{\rho_a}{u_a} = \frac{\rho_2}{u_2}$. The contact discontinuity J_{1a} is heading to the point $(\xi, \eta) = (u_1, u_1)$ and the rarefaction wave R_{a2} is heading to the point ($2u$, $2u$) for $u_2 \le u \le u_1$. The contact discontinuity J_{2b} and the shock S_{b3} – which are both parallel to the negative ξ-axis – and a new state (u_b, ρ_b) between J_{2b} and S_{b3} are formed. The state (u_b, ρ_b) satisfies $u_b = u_2$ and $\frac{\rho_b}{u_b} = \frac{\rho_3}{u_3}$. The contact discontinuity J_{2b} is heading to the point (u_2, u_2) and the shock S_{b3} is heading to the point $(u_2 + u_3, u_2 + u_3)$. The shock S_{3c} and the contact discontinuity J_{c1} – which are both parallel to the positive ξ-axis – and a new state (u_c, ρ_c) between S_{3c} and J_{c1} are formed. The state (u_c, ρ_c) satisfies $u_c = u_1$ and $\frac{\rho_c}{u_c} = \frac{\rho_3}{u_3}$. The contact discontinuity J_{c1} is heading to the point (u_1, u_1) and the shock S_{3c} is heading to the point $(u_1 + u_3, u_1 + u_3)$. The contact discontinuity J_{2b} intersects with R_{a2} at the point $(\xi_0, \eta_0) = (2u_2, u_2)$. This contact discontinuity J_{2b} penetrates the whole rarefaction wave R_{a2} to form a contact discontinuity $\eta = \eta(\xi)$ satisfying the Rankine–Hugoniot relation from the

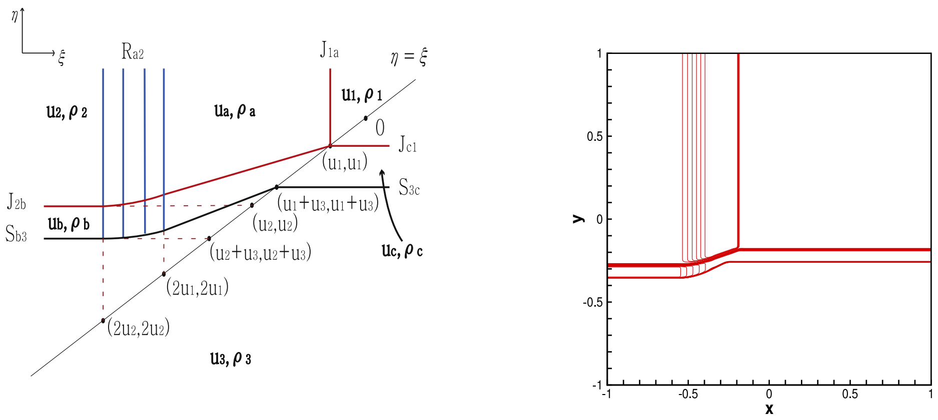

(a) analytic solution (b) numerical solution

Fig. 3. Case 2. $JR + JS + SJ$ $(u_2 < u_1 < u_3 < 0)$.

point $(\xi_0, \eta_0) = (2u_2, u_2)$,

$$\begin{cases} \dfrac{d\eta}{d\xi} = \dfrac{\eta - u}{\xi - u}, \\ \xi = 2u, \\ \dfrac{\rho}{u} = \dfrac{\rho_2}{u_2},\ u_2 \le u \le u_1, \\ (\xi_0, \eta_0) = (2u_2, u_2), \end{cases} \tag{37}$$

which gives

$$\eta = \xi - \frac{\xi^2}{4u_2}, \quad 2u_2 \le \xi \le 2u_1. \tag{38}$$

This contact discontinuity continues from $(2u_1, \frac{2u_1u_2 - u_1^2}{u_2})$ to (u_1, u_1) and it has the form as

$$\eta - u_1 = \frac{u_2 - u_1}{u_2}(\xi - u_1). \tag{39}$$

This contact discontinuity meets two contact discontinuities J_{1a} and J_{c1} at their singular point (u_1, u_1). On the other hand, the shock S_{b3} meets the rarefaction waves $R_{bc}(= R_{a2})$ at the point $(\xi_1, \eta_1) = (2u_2, u_2 + u_3)$, then the shock $\eta = \eta(\xi)$ satisfies

$$\begin{cases} \dfrac{d\eta}{d\xi} = \dfrac{\eta - (u + u_3)}{\xi - (u + u_3)}, \\ \xi = 2u, \\ \dfrac{\rho}{u} = \frac{\rho_2}{u_2},\ u_2 \le u \le u_1, \\ (\xi_1, \eta_1) = (2u_2, u_2 + u_3), \end{cases} \tag{40}$$

which gives

$$\eta = \xi - \frac{1}{u_2 - u_3}\left(\frac{\xi}{2} - u_3\right)^2, \quad 2u_2 \le \xi \le 2u_1. \tag{41}$$

This shock continues from the point $(2u_1, \frac{2u_1u_2 - u_1^2 - u_3^2}{u_2 - u_3})$ to $(u_1 + u_3, u_1 + u_3)$ and it has the form as

$$\eta - (u_1 + u_3) = \frac{u_2 - u_1}{u_2 - u_3}(\xi - (u_1 + u_3)). \tag{42}$$

This shock meets S_{3c} at their singular point $(u_1 + u_3, u_1 + u_3)$. The analytic solution and the numerical solution are shown in Fig. 3(a) and (b), respectively. The initial condition for this case is $u_1 = -0.37$, $u_2 = -0.56$, $u_3 = -0.15$.

Case 3. $RJ + SJ + JS$

In this case, the initial states satisfy $0 < u_2 < u_1 < u_3$. After the exterior waves are formed from each initial discontinuity, the contact discontinuity J_{a2} intersects with S_{2b} at the point $(u_2, u_2 + u_3)$. Then the contact discontinuity J_{cb} meets two contact discontinuities J_{b3} and J_{3c} at their singular point (u_3, u_3). The shock $S_{ac}(= S_{2b})$ intersects with R_{1a} at the point $(\xi_0, \eta_0) = (2u_2, u_2 + u_3)$. This shock penetrates the whole rarefaction wave R_{1a} to form a curved shock $\eta = \eta(\xi)$ which can

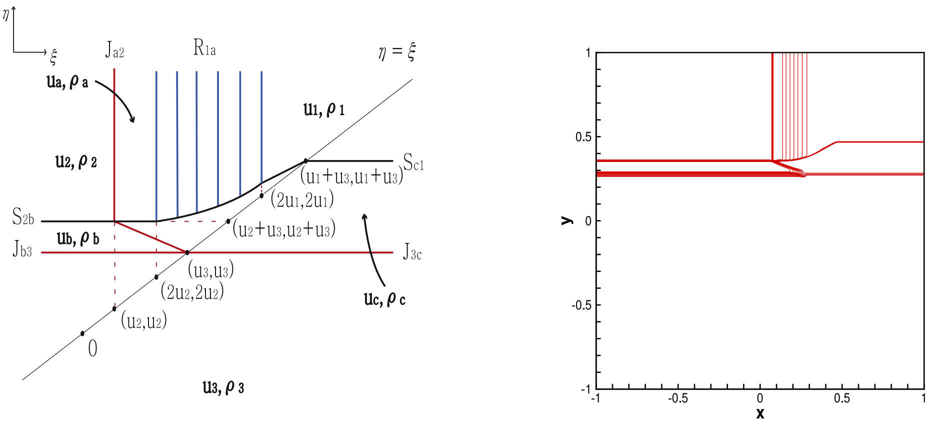

(a) analytic solution (b) numerical solution

Fig. 4. Case 3. $RJ + SJ + JS$ $(0 < u_2 < u_1 < u_3)$.

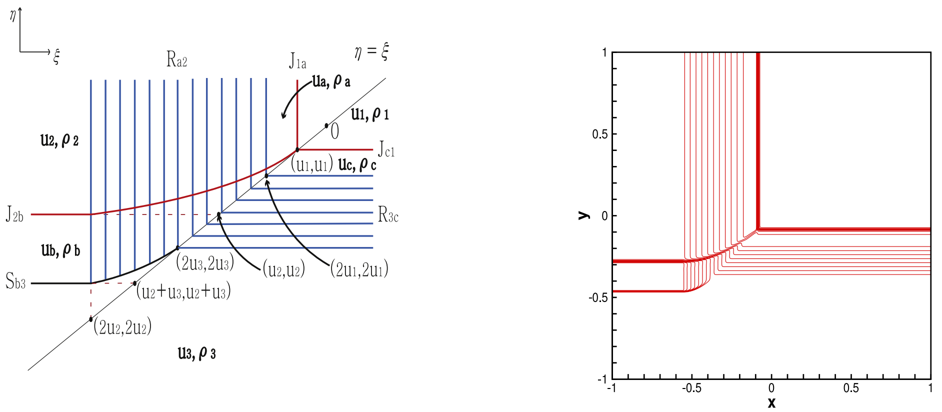

(a) analytic solution (b) numerical solution

Fig. 5. Case 4. $JR + JS + RJ$ $(u_2 < u_3 < u_1 < 0)$.

be calculated similar to case 2. Then a straight shock continues from $(2u_1, 2u_1 - \frac{(u_1-u_3)^2}{u_2-u_3})$ to $(u_1 + u_3, u_1 + u_3)$. This shock meets S_{c1} at their singular point $(u_1 + u_3, u_1 + u_3)$. The analytic solution and the numerical solution are shown in Fig. 4(a) and (b), respectively. The initial condition for this case is $u_1 = 0.37$, $u_2 = 0.15$, $u_3 = 0.56$.

5.1.3. One shock

Case 4. $JR + JS + RJ$

In this case, the initial states satisfy $u_2 < u_3 < u_1 < 0$. After the exterior waves are formed from each initial discontinuity, the contact discontinuity J_{2b} intersects with R_{a2} at the point $(\xi_0, \eta_0) = (2u_2, u_2)$. Then the contact discontinuity J_{2b} penetrates the whole rarefaction wave R_{a2}. This contact discontinuity continues from the point $(2u_1, \frac{2u_1u_2-u_1^2}{u_2})$ to $(u_1,\ u_1)$ and meets two contact discontinuities J_{1a} and J_{c1} at their singular point $(u_1,\ u_1)$. The shock S_{b3} meets the rarefaction waves R_{a2} at the point $(\xi_1, \eta_1) = (2u_2, u_2 + u_3)$, then the curved shock stops at the point $(2u_3,\ 2u_3)$. On the other hand, both rarefaction waves R_{a2} and R_{3c} meet at the same singular point $(2u,\ 2u)$ for $u_3 \le u \le u_1$. The analytic solution and the numerical solution are shown in Fig. 5(a) and (b), respectively. The initial condition for this case is $u_1 = -0.17$, $u_2 = -0.56$, $u_3 = -0.37$.

Case 5. $R + JS + R$

In this case, the initial states satisfy $u_2 < u_3 < 0 < u_1$. After the planar waves are formed from each initial discontinuity, the contact discontinuity J_{2b} intersects with R_{12} at the point $(\xi_0, \eta_0) = (2u_2, u_2)$. J_{2b} penetrates the rarefaction wave R_{12} and it ends at the point (0, 0). The shock S_{b3} meets the rarefaction waves R_{12} at the point $(\xi_1, \eta_1) = (2u_2, u_2 + u_3)$, then the curved shock $\eta = \eta(\xi)$ stops at the point $(2u_3,\ 2u_3)$. Two rarefaction waves R_{12} and R_{31} meet at the same singular point $(2u,\ 2u)$ for $u_3 \le u \le u_1$. The analytic solution and the numerical solution are shown in Fig. 6(a) and (b), respectively. The initial condition for this case is $u_1 = 0.17$, $u_2 = -0.56$, $u_3 = -0.37$.

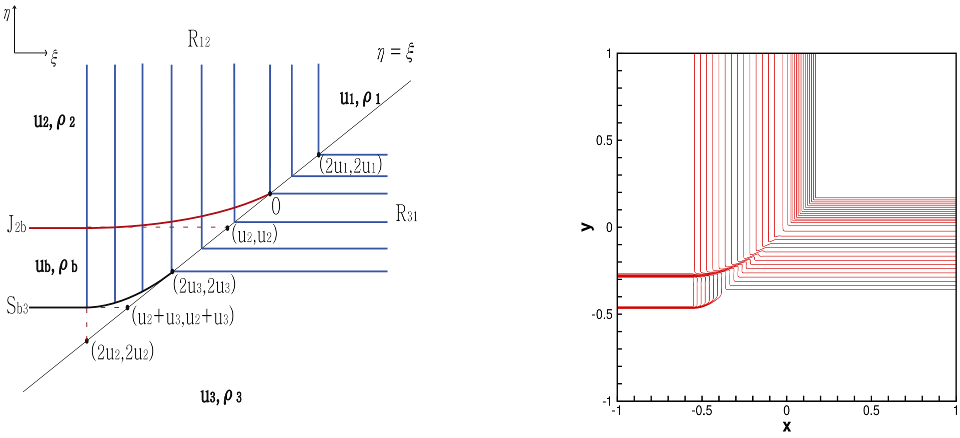

(a) analytic solution (b) numerical solution

Fig. 6. Case 5. $R+JS+R$ ($u_2<u_3<0<u_1$).

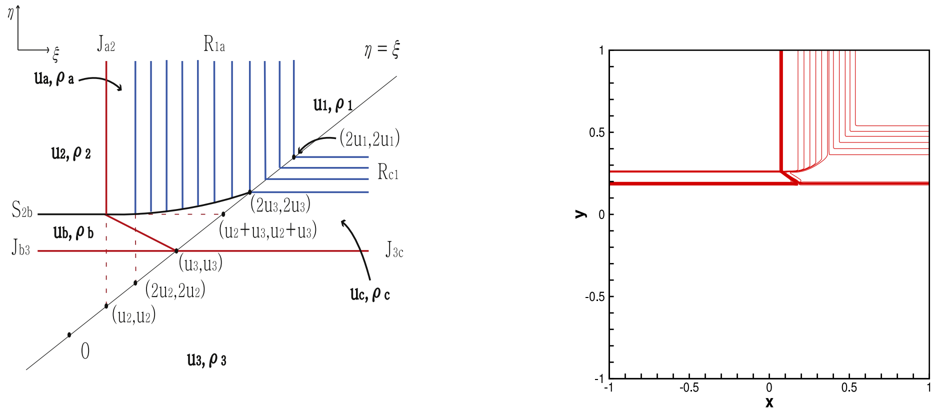

(a) analytic solution (b) numerical solution

Fig. 7. Case 6. $RJ+SJ+JR$ ($0<u_2<u_3<u_1$).

Case 6. $RJ+SJ+JR$

In this case, the initial states satisfy $0<u_2<u_3<u_1$. After the planar waves are formed from each initial discontinuity, the contact discontinuity J_{a2} intersects with S_{2b} at the point (u_2, u_2+u_3). Then the contact discontinuity J_{cb} meets two contact discontinuities J_{b3} and J_{3c} at their singular point $(u_3,\ u_3)$. The shock $S_{ac}(=S_{2b})$ meets the rarefaction waves R_{1a} at the point $(\xi_0, \eta_0)=(2u_2, u_2+u_3)$, then the curved shock $\eta=\eta(\xi)$ stops at the point $(2u_3,\ 2u_3)$. Two rarefaction waves R_{1a} and R_{c1} meet at the same singular point $(2u,\ 2u)$ for $u_3\le u\le u_1$. The analytic solution and the numerical solution are shown in Fig. 7(a) and (b), respectively. The initial condition for this case is $u_1=0.56,\ u_2=0.15,\ u_3=0.37$.

5.1.4. No shock

Case 7. $JR+JR+RJ$

In this case, the initial states satisfy $u_3<u_2<u_1<0$. After the planar waves are formed from each initial discontinuity, the contact discontinuity J_{2b} intersects with R_{a2} at the point $(\xi_0, \eta_0)=(2u_2, u_2)$, then the contact discontinuity $\eta=\eta(\xi)$ satisfies the Rankine–Hugoniot relation. This contact discontinuity continues from the point $(2u_1, \frac{2u_1u_2-u_1^2}{u_2})$ to $(u_1,\ u_1)$ and it meets two contact discontinuities J_{1a} an J_{c1} at the point $(u_1,\ u_1)$. Two rarefaction waves R_{b3} and R_{3c} meet at the same singular point $(2u,\ 2u)$ where $u_3\le u\le u_2$. The analytic solution and the numerical solution are shown in Fig. 8(a) and (b), respectively. The initial condition for this case is $u_1=-0.12,\ u_2=-0.37,\ u_3=-0.56$.

Case 8. $R+JR+R$

In this case, the initial states satisfy $u_3<u_2<0<u_1$. After the planar waves are formed from each initial discontinuity, the contact discontinuity J_{2b} intersects with R_{12} at the point $(\xi_0, \eta_0)=(2u_2, u_2)$, then this curved contact discontinuity ends at the point (0, 0). Rarefaction waves R_{12} and R_{31} meet at the same singular point $(2u,\ 2u)$ where $u_2\le u\le u_1$ and R_{b3} and

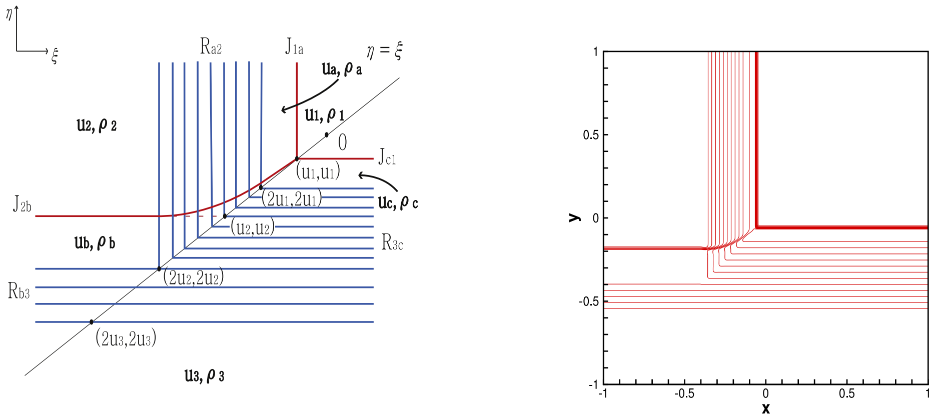

(a) analytic solution (b) numerical solution

Fig. 8. Case 7. $JR + JR + RJ$ ($u_3 < u_2 < u_1 < 0$).

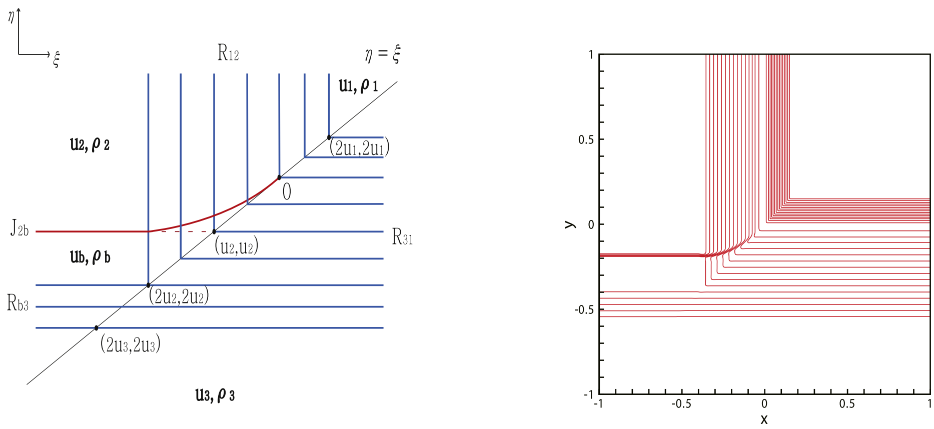

(a) analytic solution (b) numerical solution

Fig. 9. Case 8. $R + JR + R$ ($u_3 < u_2 < 0 < u_1$).

R_{31} meet at $(2u, 2u)$ where $u_3 \le u \le u_2$. The analytic solution and the numerical solution are shown in Fig. 9(a) and (b), respectively. The initial condition for this case is $u_1 = 0.15$, $u_2 = -0.37$, $u_3 = -0.56$.

5.2. One delta shock

Case 9. $S_\delta + R + RJ$

In this case, the initial states satisfy $u_3 < u_1 < 0 < u_2$. The exterior wave connecting states (u_1, ρ_1) and (u_2, ρ_2) is the delta shock $S_{\delta_{12}}$ parallel to η-axis. The delta shock $S_{\delta_{12}}$ is heading to the point $(u_1 + u_2, u_1 + u_2)$. The exterior wave connecting states (u_2, ρ_2) and (u_3, ρ_3) are the rarefaction wave R_{23} parallel to ξ-axis. The rarefaction wave R_{23} is heading to the point $(2u, 2u)$ for $u_3 \le u \le u_2$. The exterior wave connecting states (u_3, ρ_3) and (u_1, ρ_1) is the rarefaction wave R_{3c} and the contact discontinuity J_{c1} parallel to ξ-axis, between them is an intermediate state (u_c, ρ_c). The state (u_c, ρ_c) satisfies $u_c = u_1$ and $\frac{\rho_c}{u_c} = \frac{\rho_3}{u_3}$. The contact discontinuity J_{c1} is heading to the point (u_1, u_1) and the rarefaction wave R_{3c} is heading to the point $(2u, 2u)$ for $u_3 \le u \le u_1$. The delta shock $S_{\delta_{12}}$ interacts with the rarefaction wave R_{23}, then a new delta shock satisfies

$$\begin{cases} \dfrac{d\eta}{d\xi} = \dfrac{\eta - (u + u_1)}{\xi - (u + u_1)}, \\ \eta = 2u, \\ \dfrac{\rho}{u} = \dfrac{\rho_2}{u_2},\ 0 \le u \le u_2, \\ (\xi_0, \eta_0) = (u_1 + u_2, 2u_2). \end{cases} \tag{43}$$

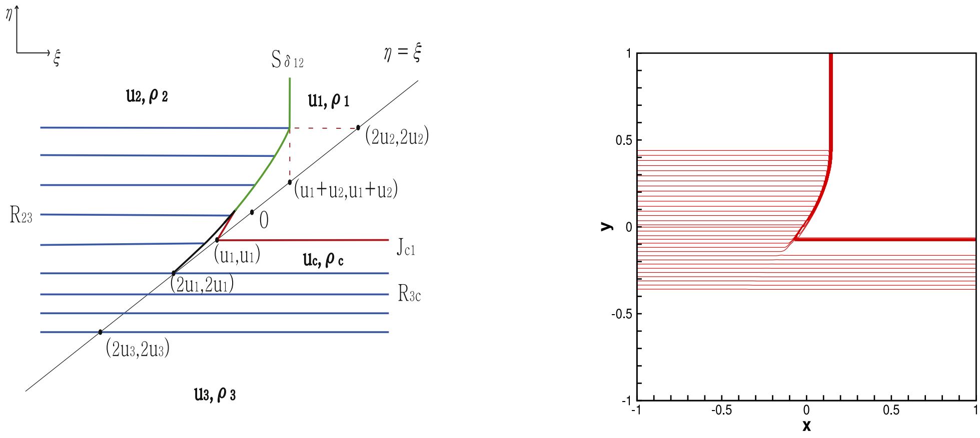

(a) analytic solution (b) numerical solution

Fig. 10. Case 9. $S_\delta + R + RJ$ ($u_3 < u_1 < 0 < u_2$).

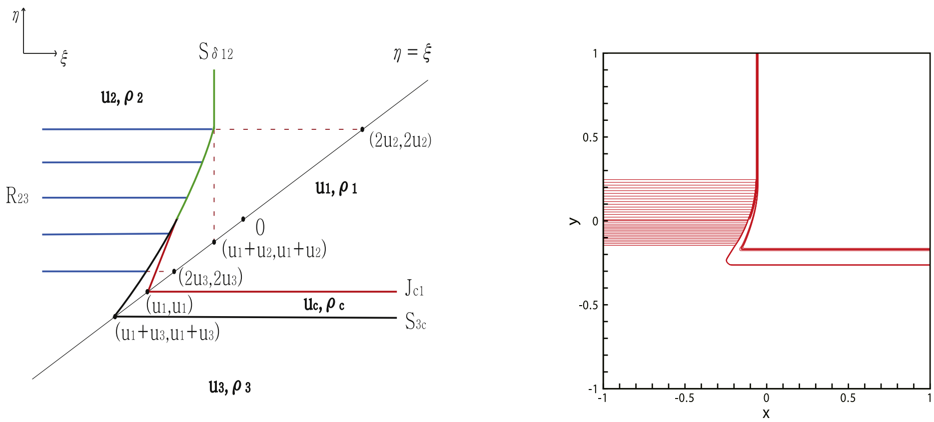

(a) analytic solution (b) numerical solution

Fig. 11. Case 10. $S_\delta + R + SJ$ ($u_1 < u_3 < 0 < u_2$).

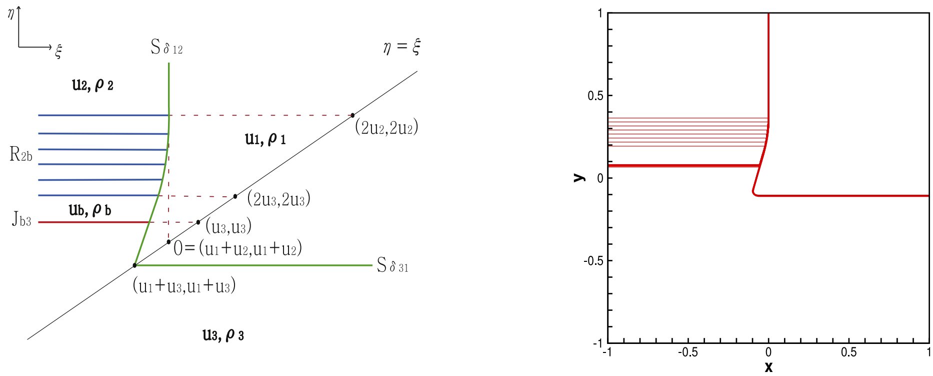

(a) analytic solution (b) numerical solution

Fig. 12. Case 11. $S_\delta + RJ + S_\delta$ ($u_1 < 0 < u_3 < u_2$).

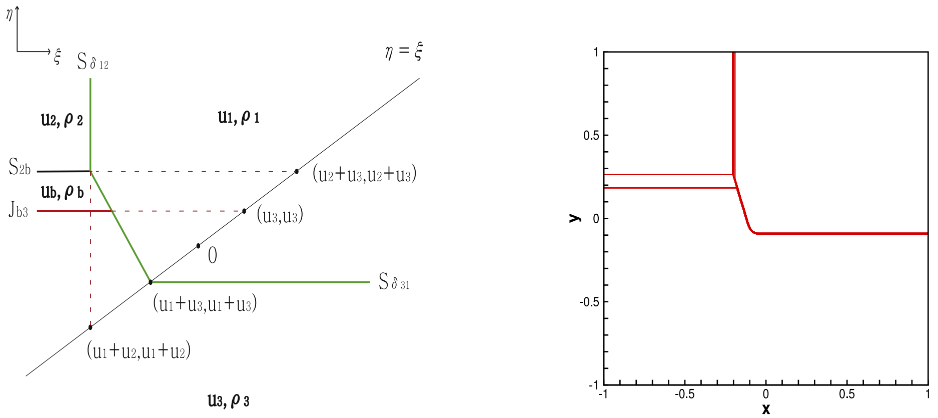

(a) analytic solution (b) numerical solution

Fig. 13. Case 12. $S_\delta + SJ + S_\delta$ $(u_1 < 0 < u_2 < u_3)$.

By integrating combined equations in (43), we obtain

$$\xi = \eta - \frac{1}{u_2 - u_1}\left(\frac{\eta}{2} - u_1\right)^2. \tag{44}$$

This delta shock ends at the point $(\xi_1, \eta_1) = (\frac{u_1^2}{u_1 - u_2}, 0)$ and then a new contact discontinuity and a new shock are formed at (ξ_1, η_1). This shock satisfies

$$\begin{cases} \dfrac{d\eta}{d\xi} = \dfrac{\eta - (u + u_1)}{\xi - (u + u_1)}, \\ \eta = 2u, \\ \dfrac{\rho}{u} = \dfrac{\rho_3}{u_3},\ u_1 \le u \le 0, \\ (\xi_1, \eta_1) = \left(\dfrac{u_1^2}{u_1 - u_2}, 0\right). \end{cases} \tag{45}$$

The similar computation shows that this shock has exactly the same form as (44) and it stops at the point $(\xi_2, \eta_2) = (2u_1, 2u_1)$. The new contact discontinuity formed at the point $(\frac{u_1^2}{u_1 - u_2}, 0)$ ends at the point (u_1, u_1) and it has the form as

$$\eta - u_1 = \frac{u_2 - u_1}{u_2}(\xi - u_1). \tag{46}$$

Two rarefaction waves meet at the same singular point $(2u, 2u)$ for $u_3 \le u \le u_1$. The analytic solution and the numerical solution are shown in Fig. 10(a) and (b), respectively. The initial condition for this case is $u_1 = -0.15,\ u_2 = 0.45,\ u_3 = -0.37$.

Case 10. $S_\delta + R + SJ$

In this case, the initial states satisfy $u_1 < u_3 < 0 < u_2$. After the planar waves are formed from each initial discontinuity, the delta shock $S_{\delta_{12}}$ interacts with the rarefaction wave R_{23}, then a curved delta shock ends at the point $(\xi_1, \eta_1) = (\frac{u_1^2}{u_1 - u_2}, 0)$. Simultaneously, a new contact discontinuity and a new shock occur at (ξ_1, η_1). This shock meets S_{3c} at their singular point $(u_1 + u_3, u_1 + u_3)$. The new contact discontinuity formed at the point (ξ_1, η_1) ends at the point (u_1, u_1). The analytic solution and the numerical solution are shown in Fig. 11(a) and (b), respectively. The initial condition for this case is $u_1 = -0.37,\ u_2 = 0.25,\ u_3 = -0.15$.

5.3. Two delta shocks

Case 11. $S_\delta + RJ + S_\delta$

In this case, the initial states satisfy $u_1 < 0 < u_3 < u_2$. After the planar waves are formed from each initial discontinuity, the delta shock $S_{\delta_{12}}$ interacts with the rarefaction wave R_{2b}, then a new delta shock stops at the point $(\xi, \eta) = (\xi_1, 2u_3)$. Then ξ_1 is $\frac{u_1^2 + u_3^2 - 2u_1 u_2}{u_1 - u_2}$. Two points $(\frac{u_1^2 + u_3^2 - 2u_1 u_2}{u_1 - u_2}, 2u_3)$ and $(u_1 + u_3, u_1 + u_3)$ are connected by the delta shock. This delta shock meets $S_{\delta_{31}}$ at their singular point $(\xi_2, \eta_2) = (u_1 + u_3, u_1 + u_3)$. The analytic solution and the numerical solution are shown in Fig. 12(a) and (b), respectively. The initial condition for this case is $u_1 = -0.37,\ u_2 = 0.37,\ u_3 = 0.15$.

Case 12. $S_\delta + SJ + S_\delta$

In this case, the initial states satisfy $u_1 < 0 < u_2 < u_3$. After the planar waves are formed from each initial discontinuity, the delta shock $S_{\delta_{12}}$ interacts with the shock S_{2b} at $(\xi_0, \eta_0) = (u_1 + u_2, u_2 + u_3)$. Two points $(u_1 + u_2, u_2 + u_3)$ and $(u_1 + u_3, u_1 + u_3)$ are connected by the delta shock. This new delta shock meets $S_{\delta_{31}}$ at their singular point $(\xi_1, \eta_1) = (u_1 + u_3, u_1 + u_3)$. The analytic solution and the numerical solution are shown in Fig. 13(a) and (b), respectively. The initial condition for this case is $u_1 = -0.56,\ u_2 = 0.15,\ u_3 = 0.37$.

Acknowledgment

We thank the anonymous referees for helpful comments and suggestions. This research was supported by Basic Research Program through the National Research Foundation of Korea (NRF) funded by the Ministry of Education (Grant No. NRF-2015R1D1A1A01057949).

References

[1] W. Hwang, W.B. Lindquist, The 2-dimensional Riemann problem for a 2 × 2 hyperbolic conservation law. I. Isotropic media., SIAM. J. Math. Anal. 34 (2003) 341–358.
[2] W. Hwang, W.B. Lindquist, The 2-dimensional Riemann problem for a 2 × 2 hyperbolic conservation law. II. Anisotropic media., SIAM. J. Math. Anal. 34 (2003) 359–384.
[3] A. Kurganov, C.T. Lin, On the reduction of numerical dissipation in central-upwind schemes., Commun. Comput. Phys. 2 (2007) 141–163.
[4] J. Li, T. Zhang, S. Yang, The Two-Dimensional Riemann Problem in Gas Dynamics., Longman, London, 1998.
[5] Y. Pang, J.P. Tian, H. Yang, Two-dimensional Riemann problem for a hyperbolic system of conservation laws in three pieces., Appl. Math. Comput. 219 (2012) 1695–1711.
[6] Y. Pang, J.P. Tian, H. Yang, Two-dimensional Riemann problem involving three J's for a hyperbolic system of nonlinear conservations laws., Appl. Math. Comput. 219 (2013) 4614–4624.
[7] Y. Pang, H. Yang, Two-dimensional Riemann problem involving three contact discontinuities for 2 × 2 hyperbolic conservation laws in anisotropic media., J. Math. Anal. Appl. 428 (2015) 77–97.
[8] C. Shen, Riemann problem for a two-dimensional quasilinear hyperbolic system, Electron. J. Differ. Equ. 237 (2015) 1–13.
[9] C. Shen, M. Sun, Z. Wang, Global structure of Riemann solutions to a system of two-dimensional hyperbolic conservation laws., Nonlinear Anal. 74 (2011) 4754–4770.
[10] M. Shin, S. Shin, W. Hwang, A treatment of contact discontinuity for central upwind scheme by changing flux functions., J. KSIAM 17 (2013) 29–45.
[11] M. Sun, Construction of the 2D Riemann solutions for a nonstrictly hyperbolic conservation law., Bull. Korean Math. Soc. 50 (2013) 201–216.
[12] D.C. Tan, T. Zhang, Two-dimensional Riemann problem for a hyperbolic system of nonlinear conservation laws I. Four-J cases., J. Differ. Equ. 111 (1994) 203–254.
[13] D.C. Tan, T. Zhang, Two-dimensional Riemann problem for a hyperbolic system of nonlinear conservation laws II. Initial data involving some rarefaction waves., J. Differ. Equ. 111 (1994) 255–282.
[14] H. Yang, Y. Zhang, New developments of delta shock waves and its applications in systems of conservation laws., J. Differ. Equ. 252 (2012) 5951–5993.
[15] T. Zhang, Y. Zheng, Conjecture on the structure of solutions of the Riemann problem for two-dimensional gas dynamics systems., SIAM J. Math. Anal. 21 (1990) 593–630.